Supporting Information for:

Depolymerization of PET by Common Alkanolamines Yields Tunable Monomers to Expand the Design Space of 3D-Printable, Self-Healing Polyamide-Ionenes

Mousumi R. Bepari, Pravin S. Shinde & Jason E. Bara*

Department of Chemical & Biological Engineering, University of Alabama, Tuscaloosa, Alabama, USA 35487-0203

Corresponding author's email address: jbara@eng.ua.edu

Table of Contents

List of Figures

S1. ^{1}H NMR of depolymerization compounds and chlorinated monomers.

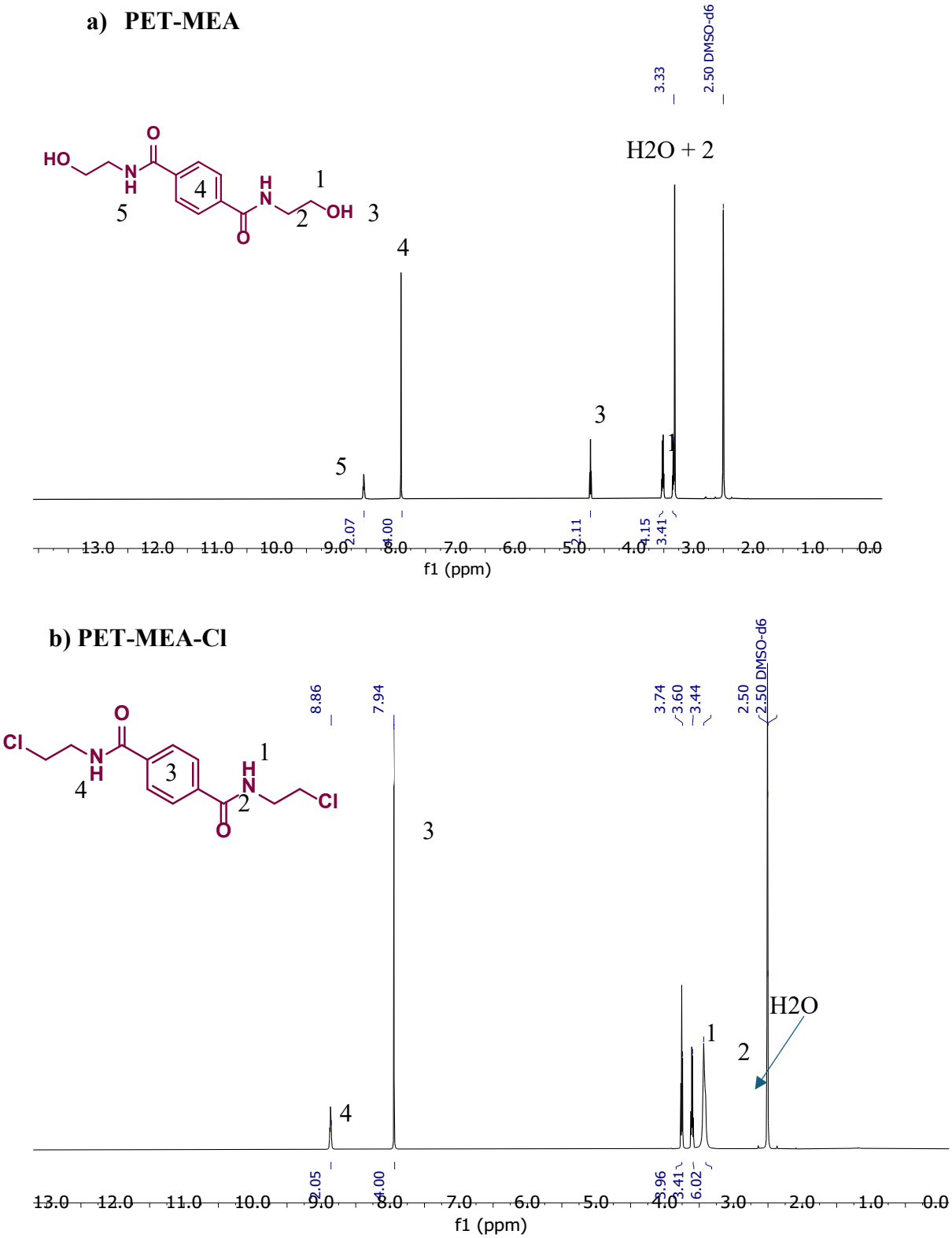

Fig. S 1 ^{1}H NMR (500MHz, d_6-DMSO) of a) PET-MEA b) PET-MEA-Cl.

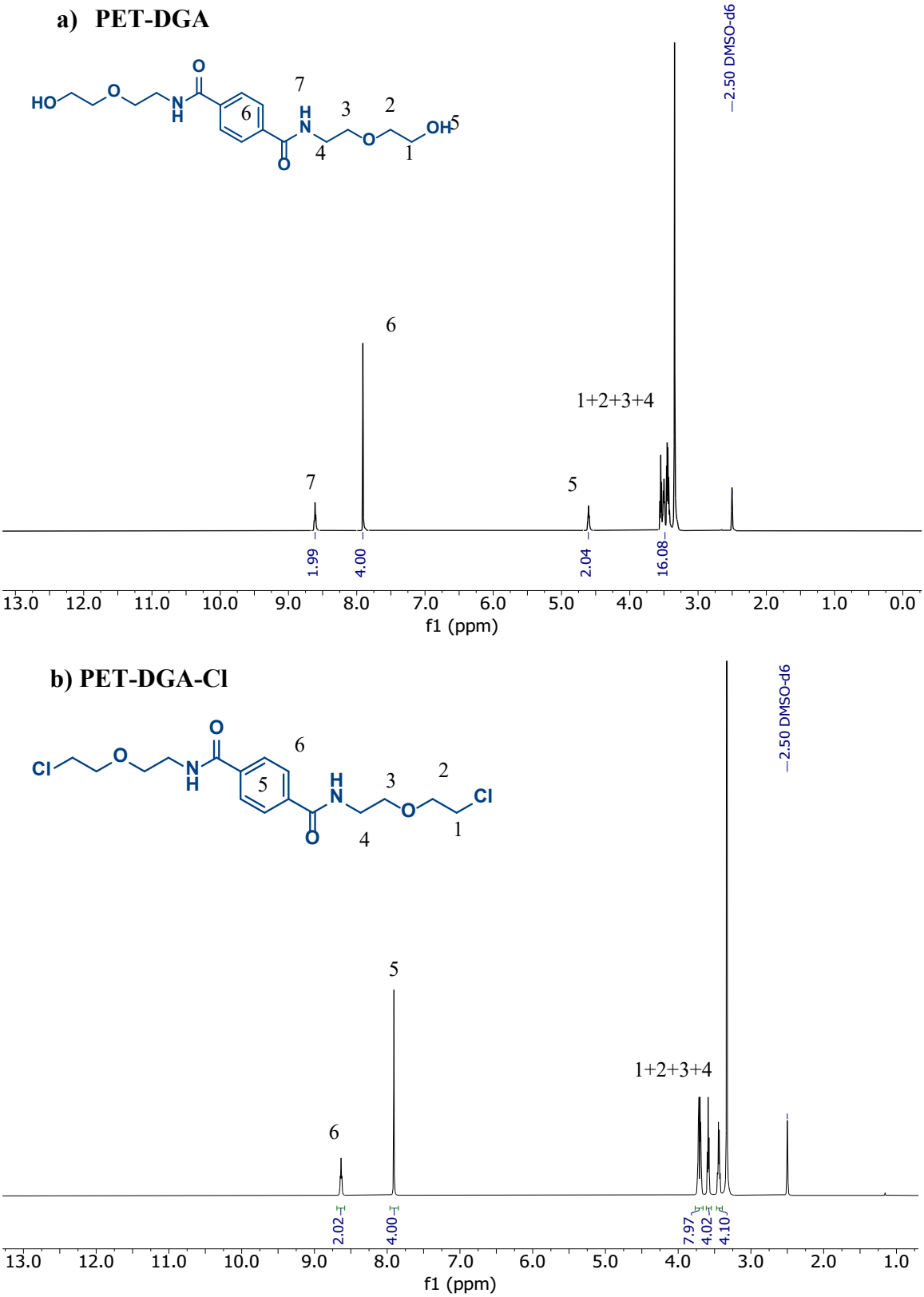

Fig. S 2 ^{1}H NMR (500MHz, d_6-DMSO) of a) PET-DGA b) PET-DGA-Cl.

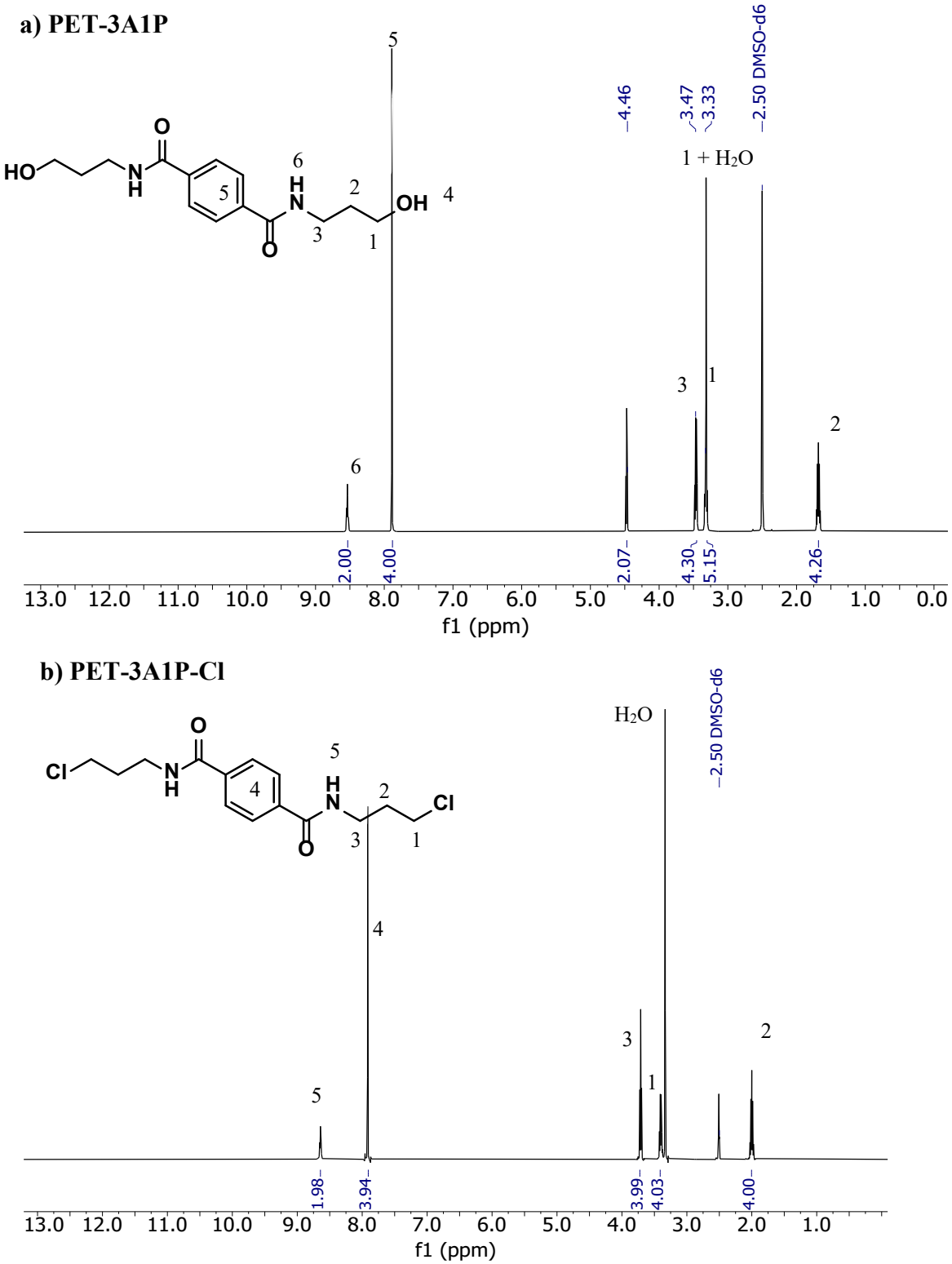

Fig. S 3 1H NMR (500MHz, d6-DMSO) of a) PET-3A1P b) PET-3A1P-Cl.

S2. Confirmation of bisimidazolium monomers by ^{1}H NMR.

a) DBH-imidazole (im-C$_6$)

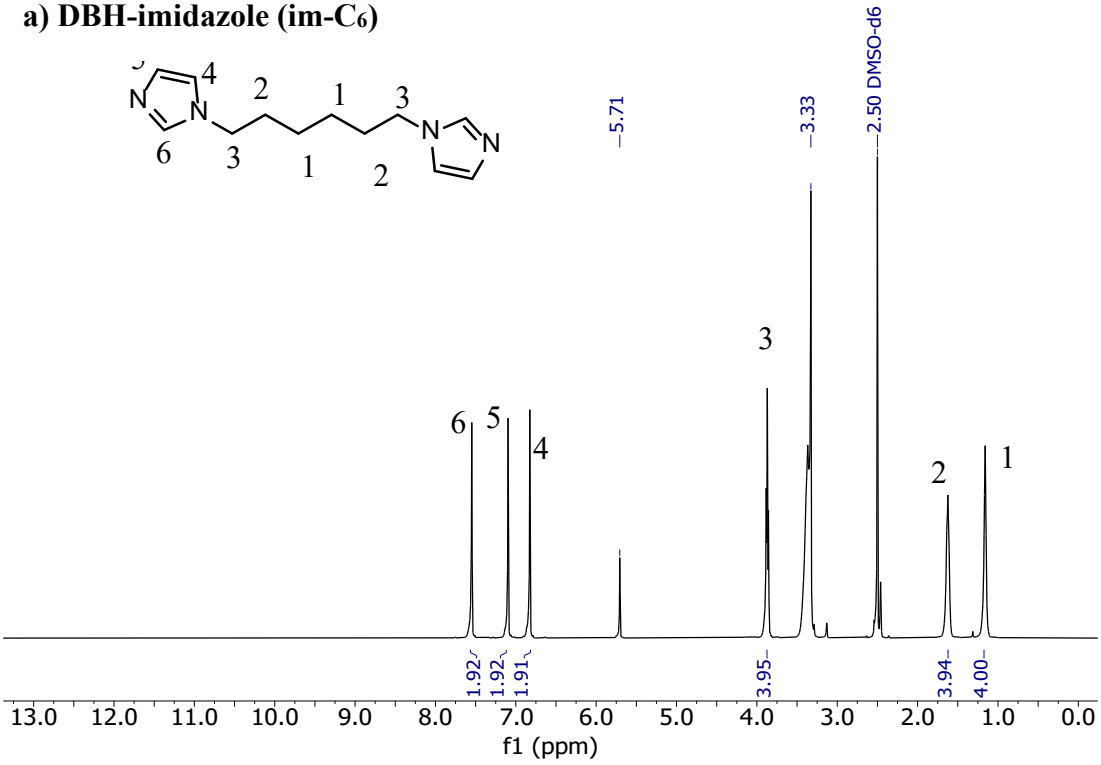

b) DBH-2methylimidazole (2mim-C$_6$)

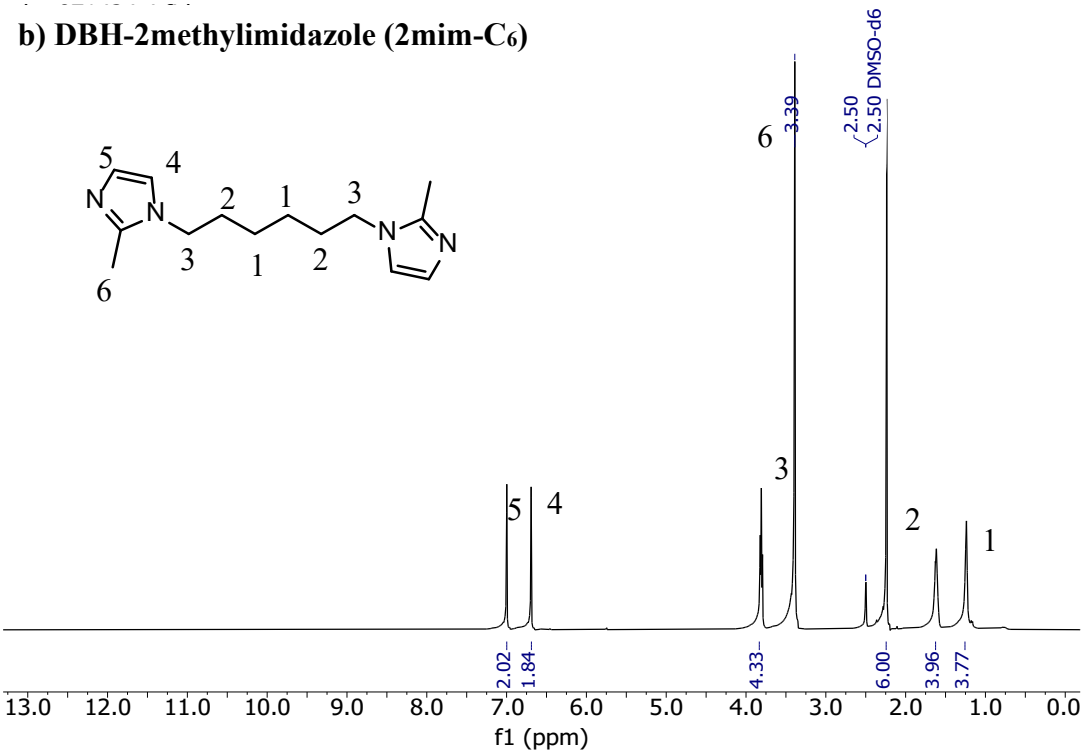

Fig. S 4 ^{1}H NMR (500MHz, d_6-DMSO) of a) 1,1'-(1,6-hexanediyl)bisimidazole (DBH_im/im-C$_6$) b) 1,1'-(1,6-hexanediyl)-2-methylbisimidazole (DBH_2mim/2mim-C$_6$).

S3. Confirmation of PA-ionenes by ^{1}H NMR.

PET-MEA-im-C_6-Tf_2N ionene (MEA-im)

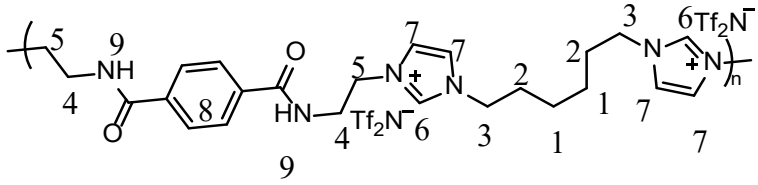

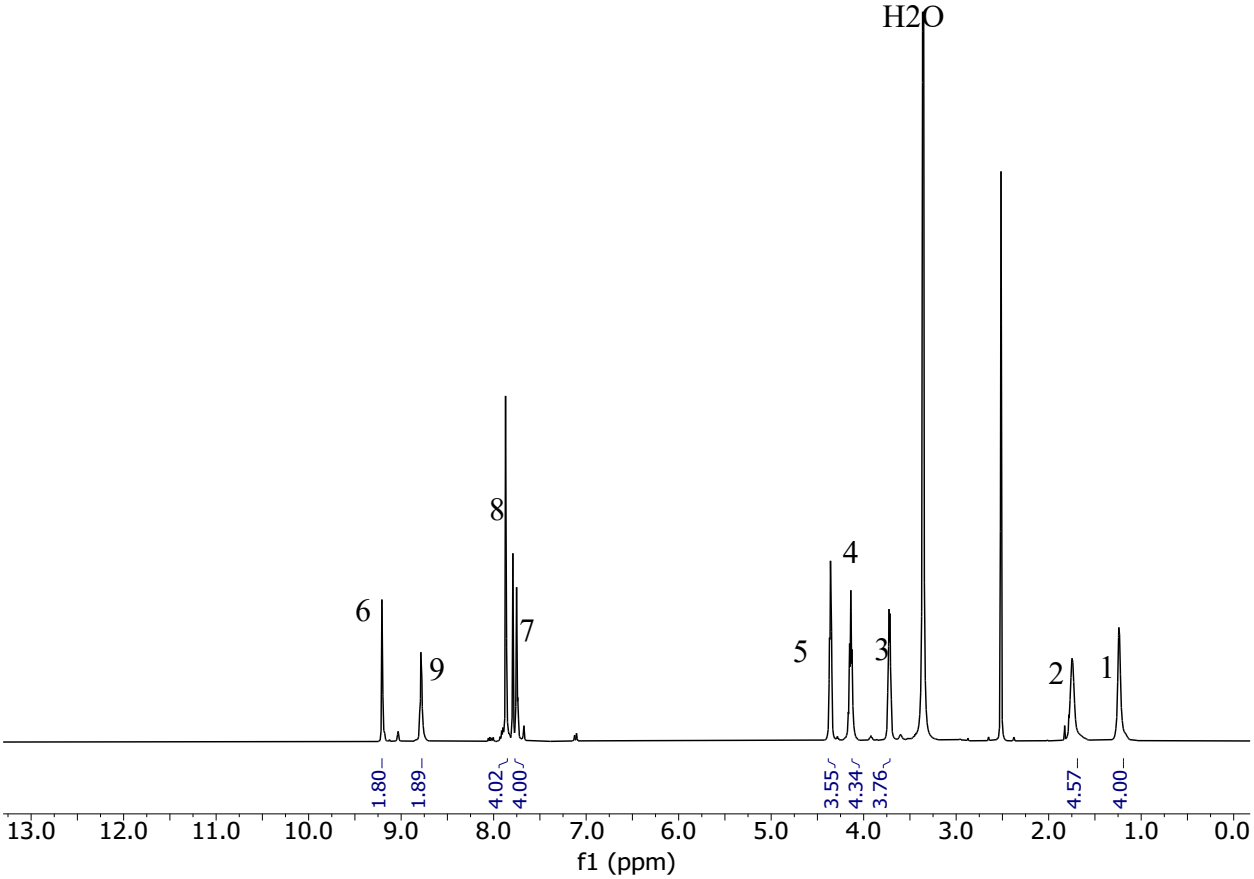

Fig. S 5 ^{1}H NMR (500MHz, d_6-DMSO) of PET-MEA-im-C_6-Tf_2N ionene.

PET-MEA-2mim-C_6-Tf_2N ionene (MEA-2mim)

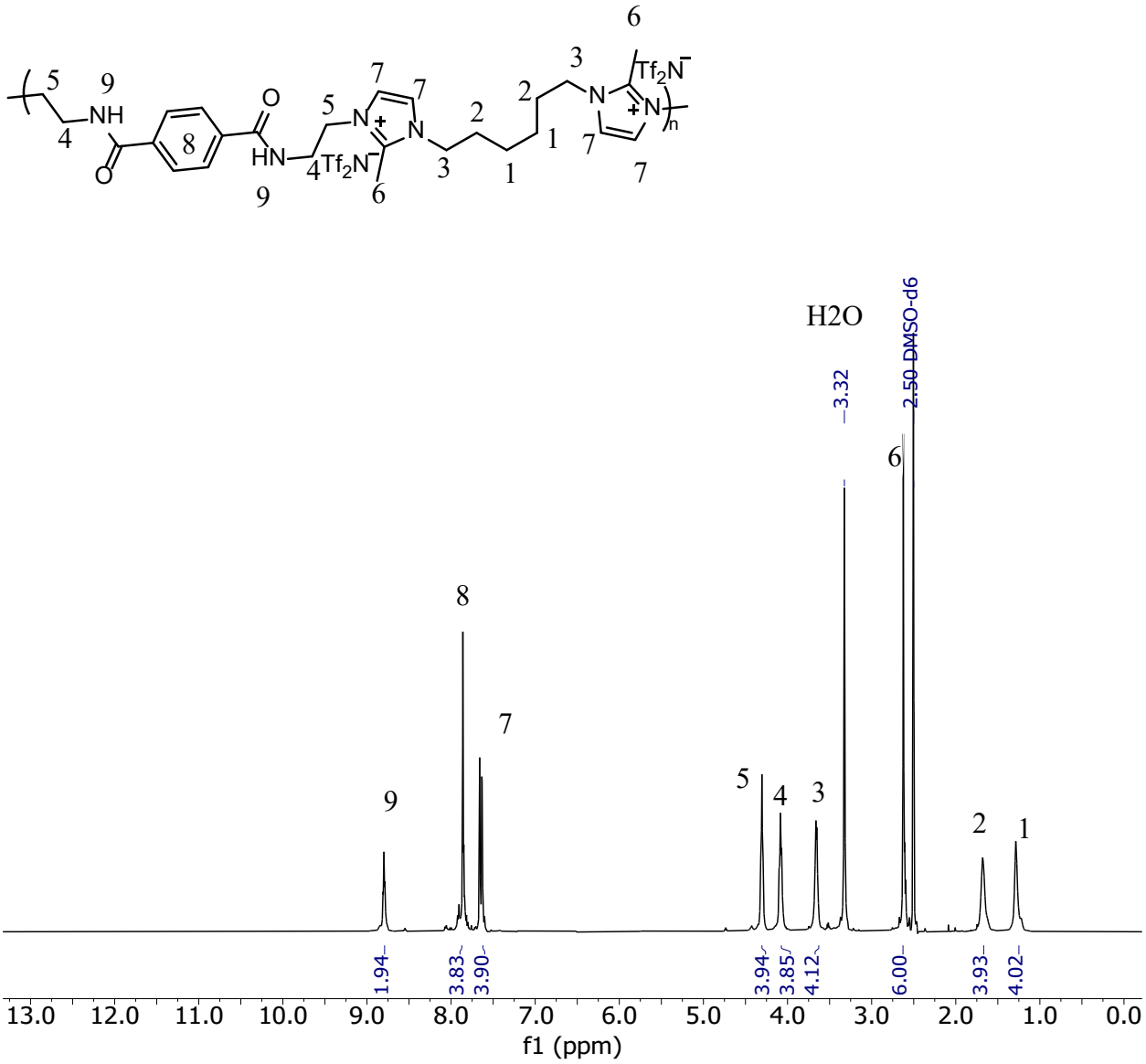

Fig. S 6 ^{1}H NMR (500MHz, d_6-DMSO) of PET-MEA-2mim-C_6-Tf_2N ionene.

PET-3A1P- im-C_6-Tf_2N ionene (3A1P-im)

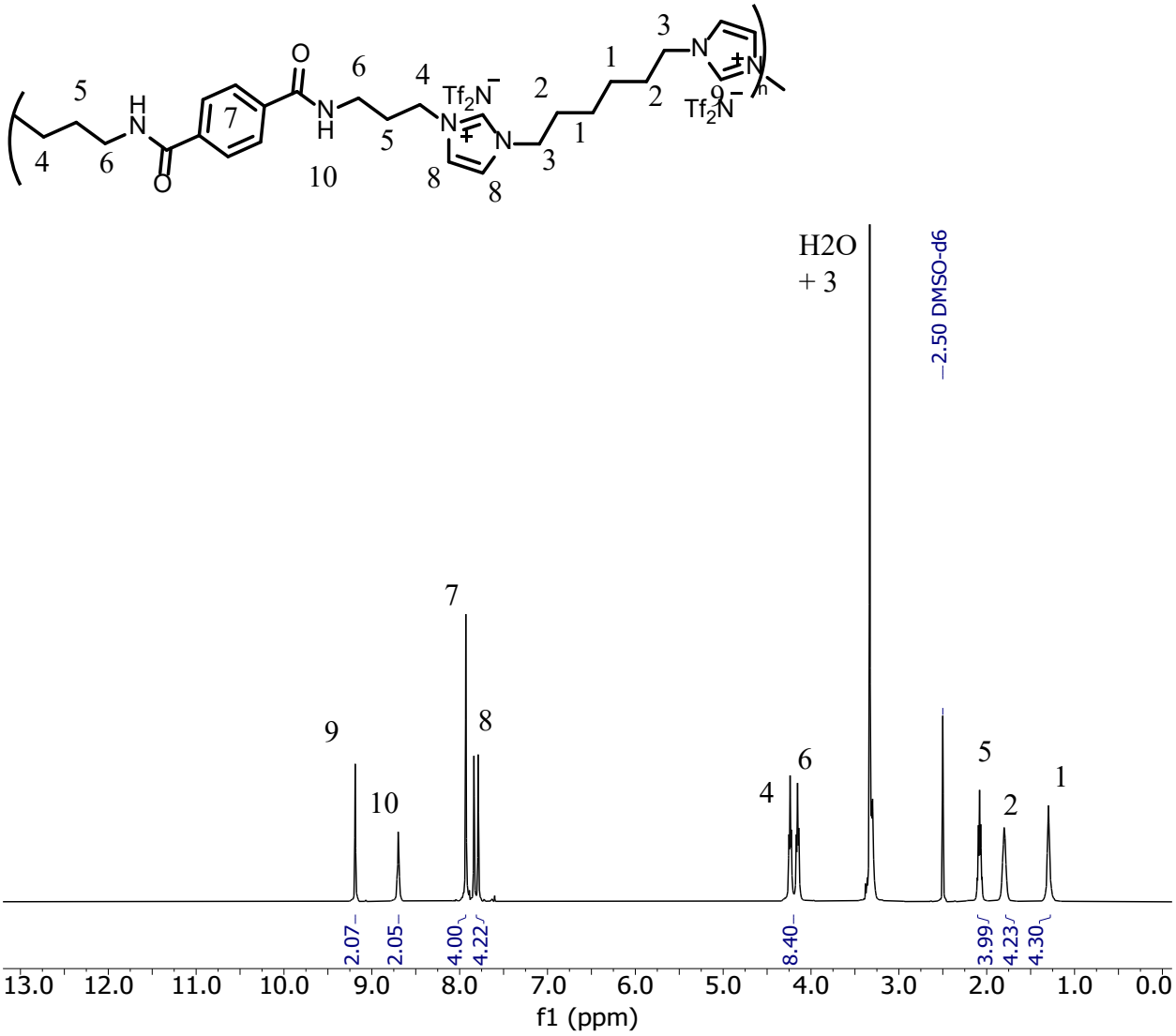

Fig. S 7 ^{1}H NMR (500MHz, d_6-DMSO) of PET-3A1P-im-C_6-Tf_2N ionene.

PET-3A1P-2mim-C_6-Tf_2N ionene (3A1P-2mim)

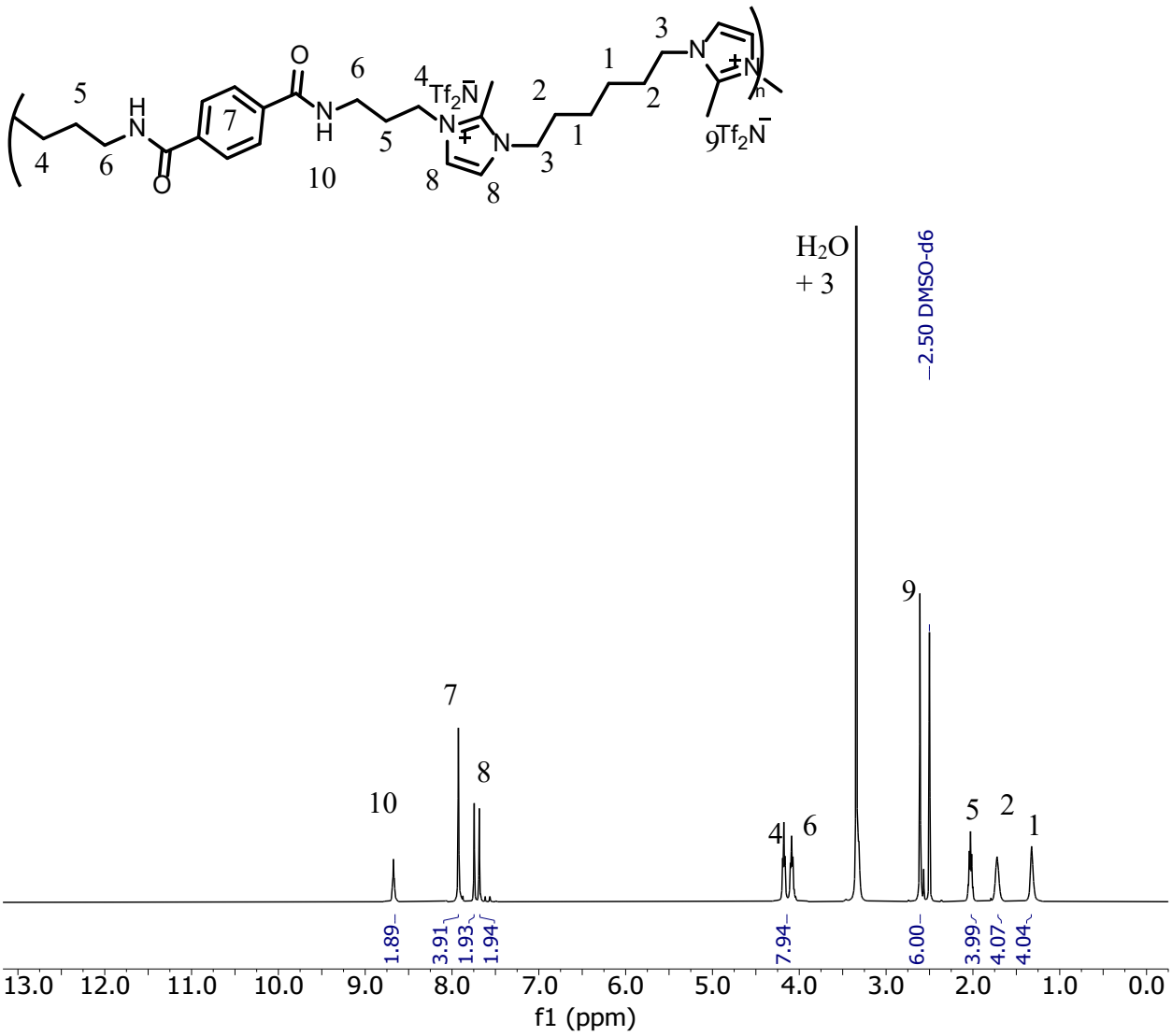

Fig. S 8 ^{1}H NMR (500MHz, d_6-DMSO) of PET-3A1P-2mim-C_6-Tf_2N ionene.

PET-DGA-im-C_6-Tf_2N ionene (DGA-im)

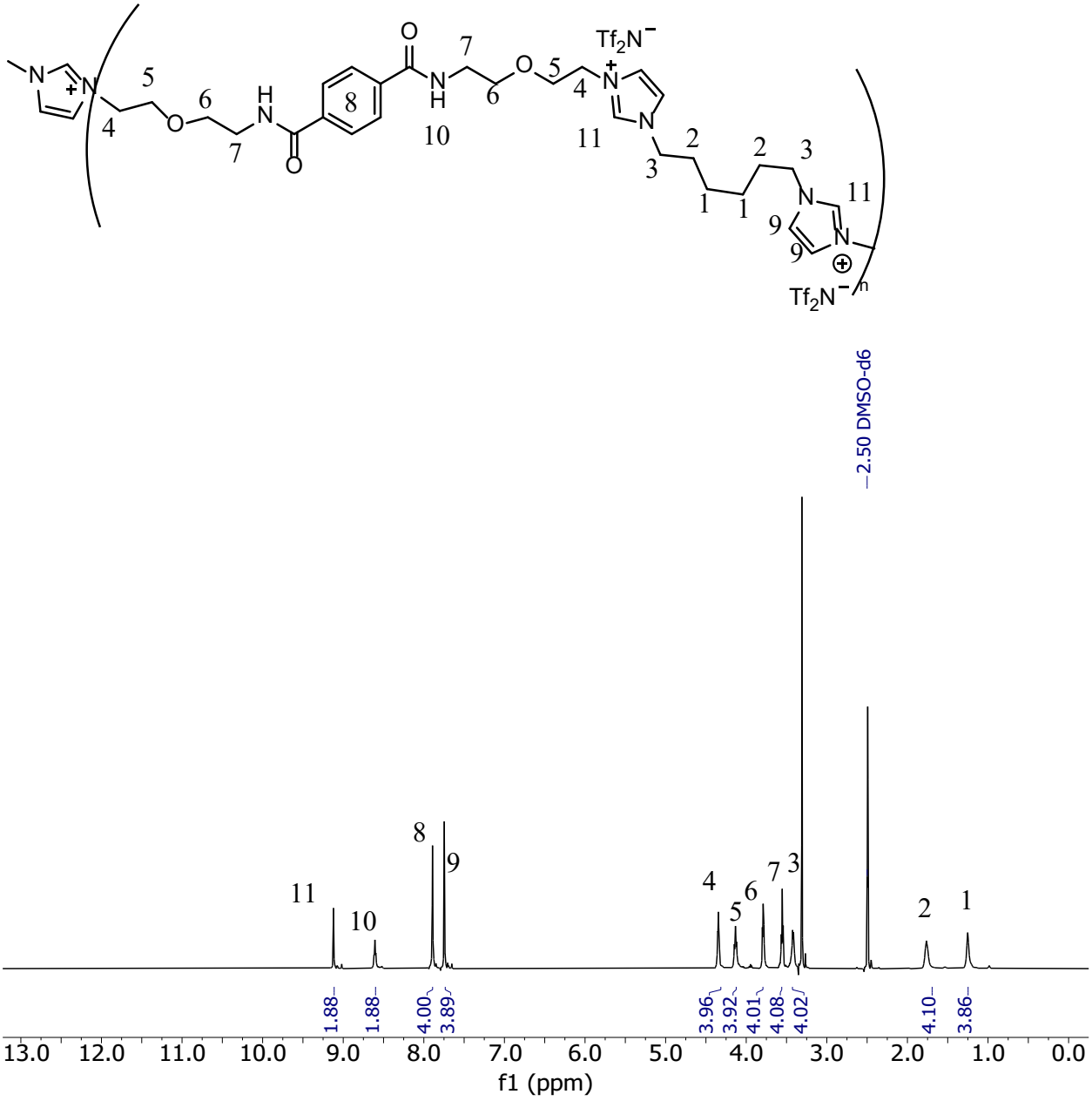

Fig. S 9 ^{1}H NMR (500MHz, d_6-DMSO) of PET-DGA-im-C_6-Tf_2N ionene.

PET-DGA-2mim-C_6-Tf_2N ionene (DGA-2mim)

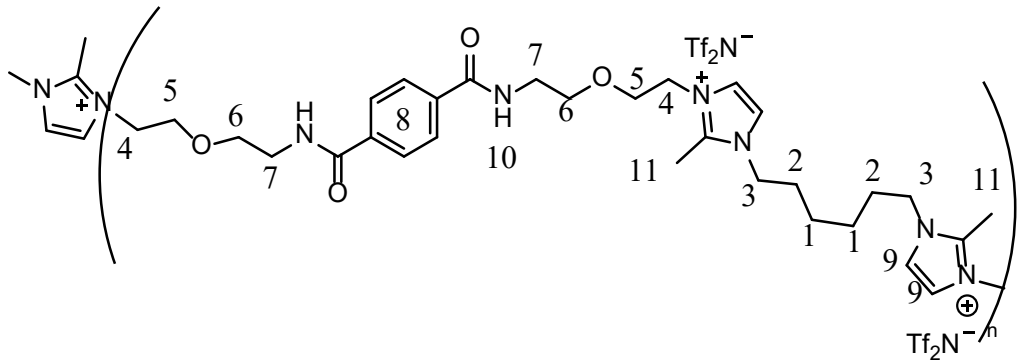

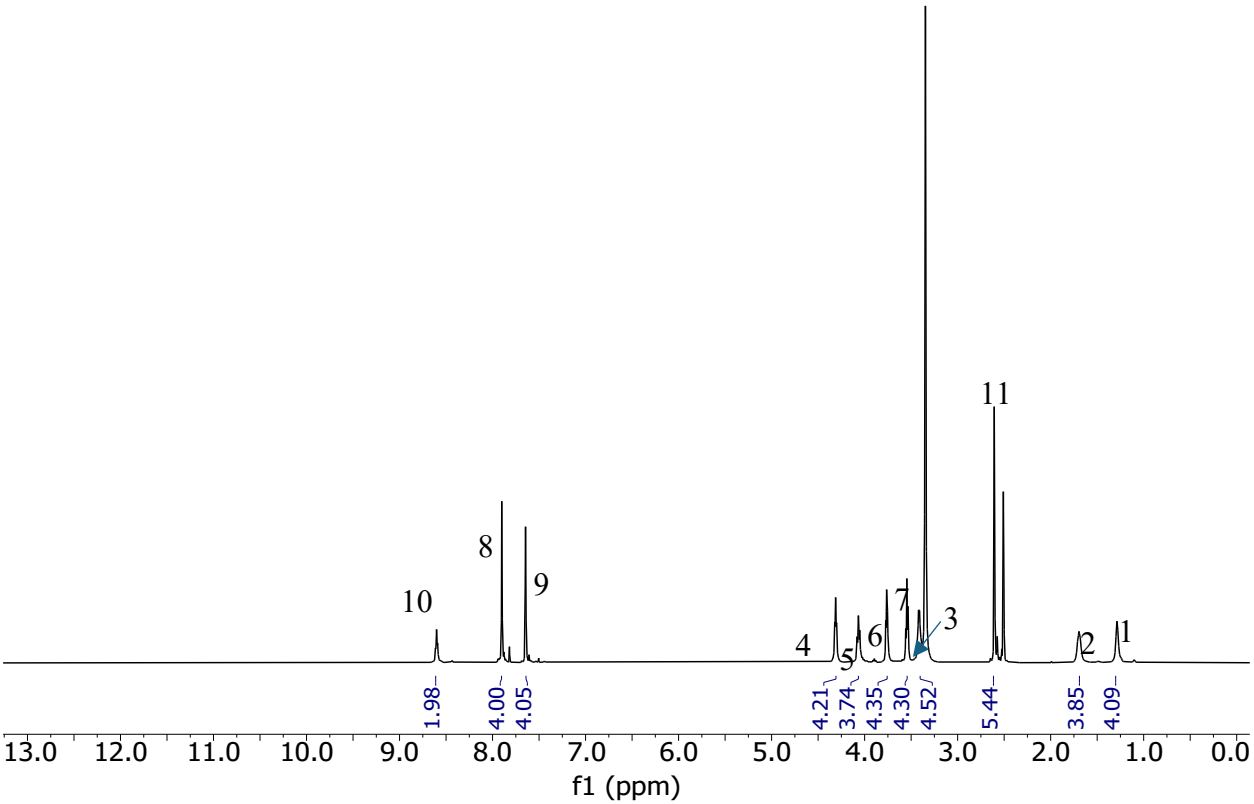

Fig. S 10 ^{1}H NMR (500MHz, d_6-DMSO) of PET-DGA-2mim-C_6-Tf_2N ionene.

S4. Structural verification of monomers (PET-MEA, PET-MEA -Cl) and corresponding polymers by FTIR.

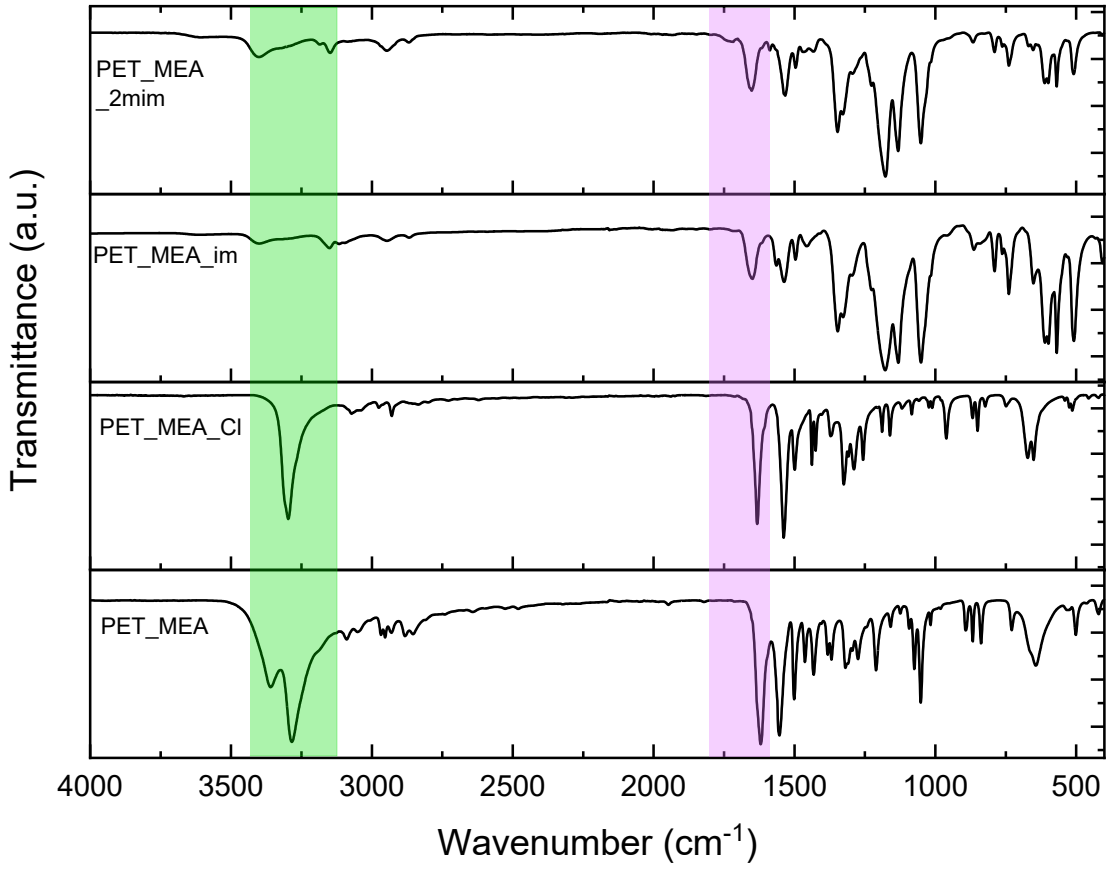

Fig. S 11 Transformation of PET-MEA compound to valuable ionene showed by ATR-FTIR.

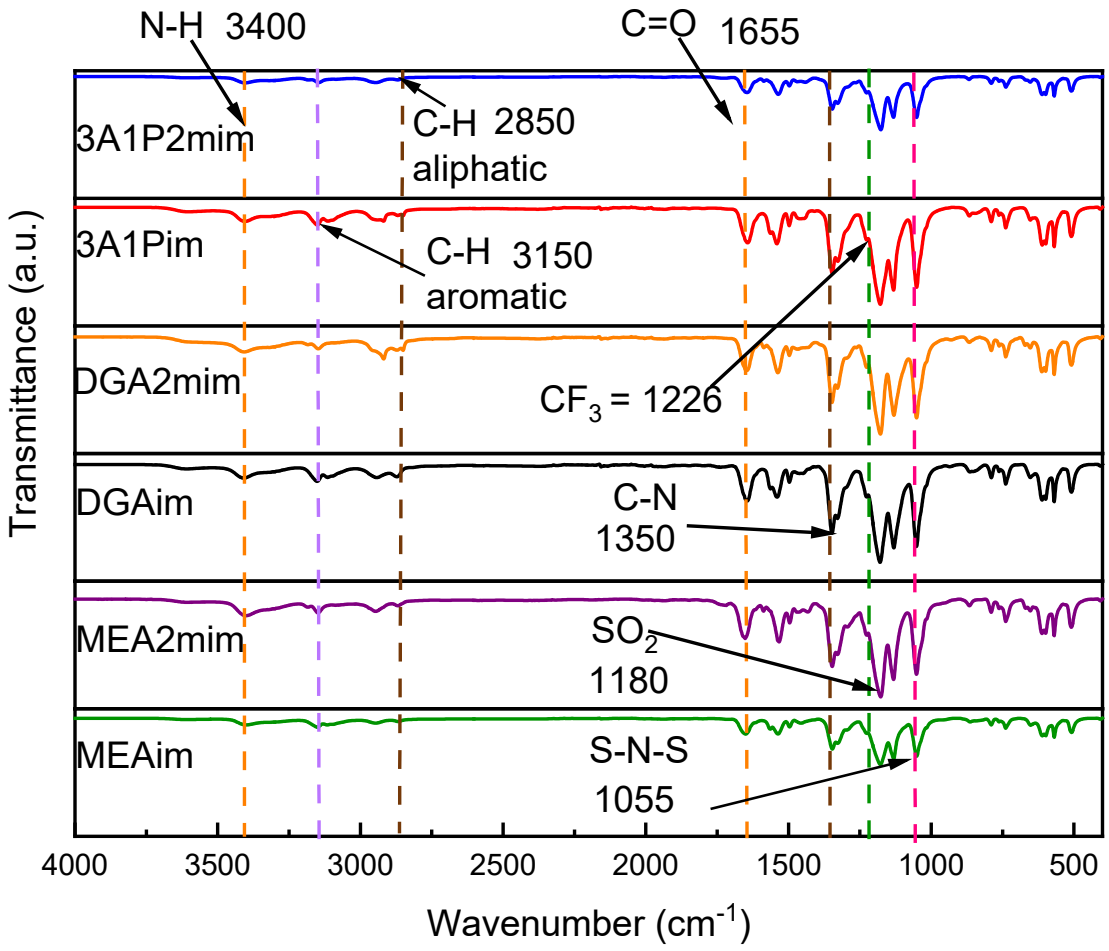

Fig. S 12 Incorporation of ionic moieties and functional groups observed in ATR-FTIR of PA-ionenes.

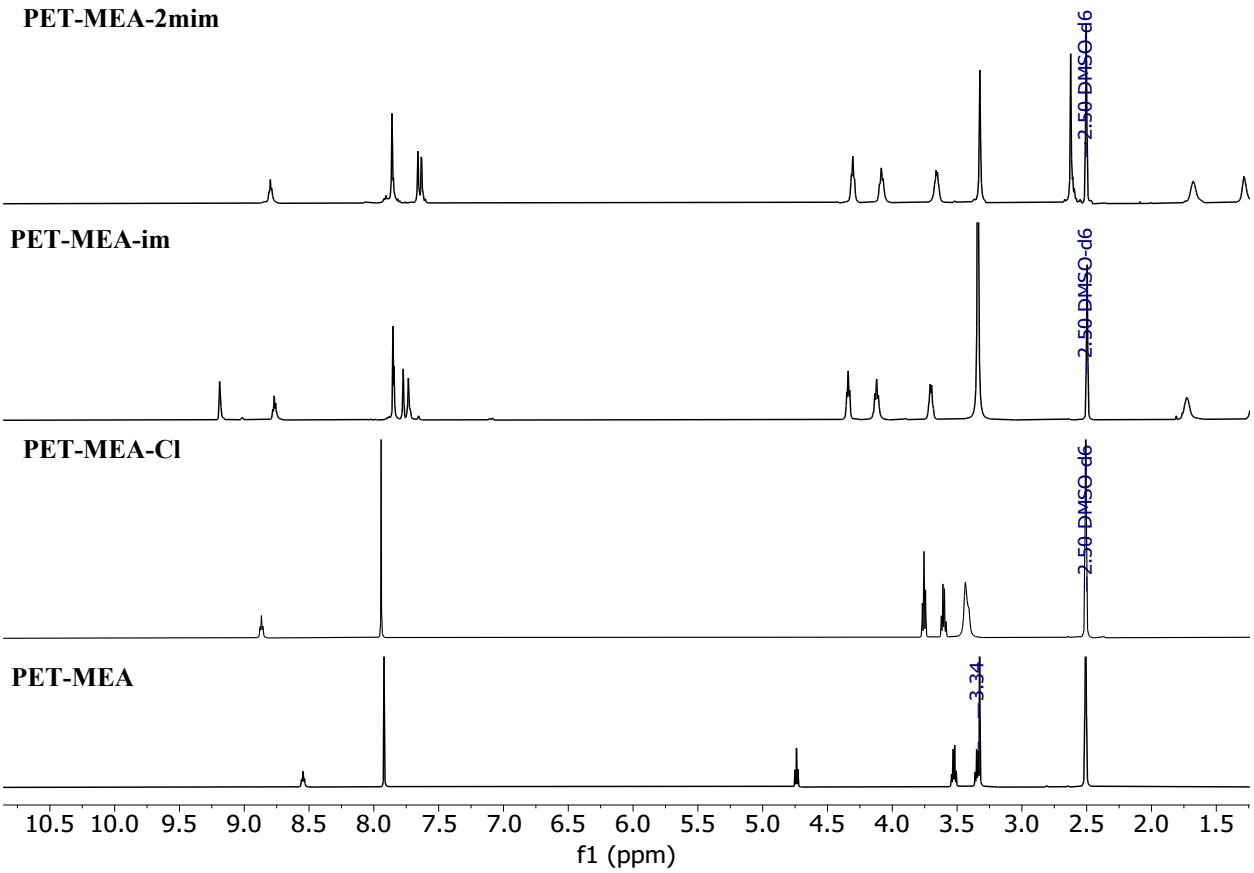

Fig. S 13 Comparison of ^{1}H NMR spectra for building blocks and final PA-ionene products "PET-MEA-im" and "PET-MEA-2mim".

S5. Thermal property (TGA, T_m), monomers composition toward ionene synthesis and printing parameters.

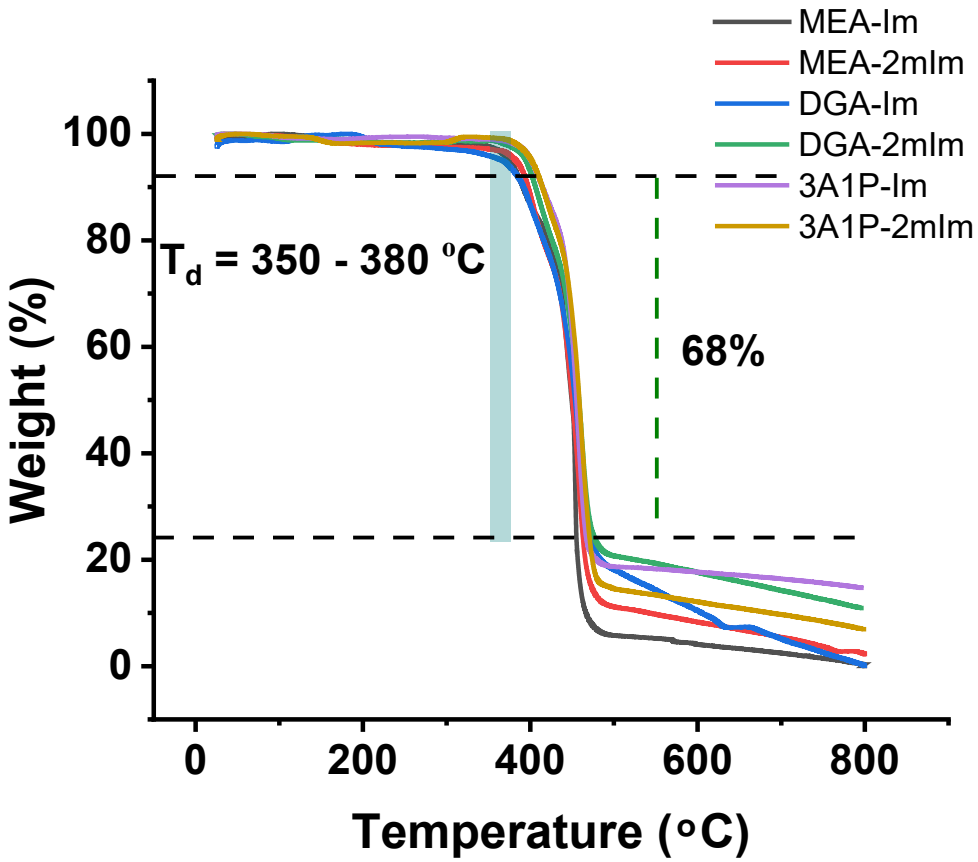

Fig. S 14 TGA plots of PA-ionenes derived from waste PET.

Table S 1. Reactant amounts and polymer yields for all six PA-ionenes

PA-Ionene	Amide dihalide	Amount	Bis-imidazole	Amount	KI	$LiTf_2N$	Ionene yield	Yield (%)
DGA_Im	PET-DGA-Cl	10 g | 26.6 mmol	C6-Im	5.8 g | 26.6 mmol	0.044 g | 0.27 mmol	14.27	21	72.7
DGA_2mIm	PET- DGA-Cl	10 g | 26.5 mmol	C6-2mIm	6.5 g | 26.5 mmol	0.044 g | 0.26 mmol	16.14	23	78
3A1P_im	PET-3A1P-Cl	8 g | 25.2 mmol	C6-Im	5.5 g | 25.2 mmol	0.04 g | 0.25 mmol	18.8	18.3	70.7
3A1P_2mim	PET-3A1P-Cl	11 g | 34.7 mmol	C6-2mIm	8.54 g | 34.7 mmol	0.06 g | 0.35 mmol	20.5	22	82.84
MEA_im	PET-MEA-Cl	8 g | 27.7 mmol	C6-Im	6.04 g | 27.7 mmol	0.045 g | 0.27 mmol	17.8	21.5	78
MEA_2mim	PET-MEA-Cl	10.5 g | 36.3 mmol	C6-2mIm	8.94 g | 36.3 mmol	0.06 g | 0.36 mmol	20.6	20.7	55.6

Table S 2. Printing parameters obtained from a 3D bioplotter.

PA-Ionene	Temperature (℃)	Speed (mm/s)	Pressure (bar)	Pre-flow (s)	Post-flow (s)
DGA-Im	72	2.5	4.7	0.2	0.05
DGA-2mIm	80	4	5.5	0.2	0.05
3A1P-im	170	4	5.5	0.2	0.05
3A1P-2mim	150	4	3.5	0.2	0.05
MEA-im	75	2.5	5.5	0.2	0.05
MEA-2mim*	180	N/A	7	0.2	0.05
(MEA-2mim) +IL	75	2.5	5.5	0.2	0.05

* The ionene was not printable at this condition*

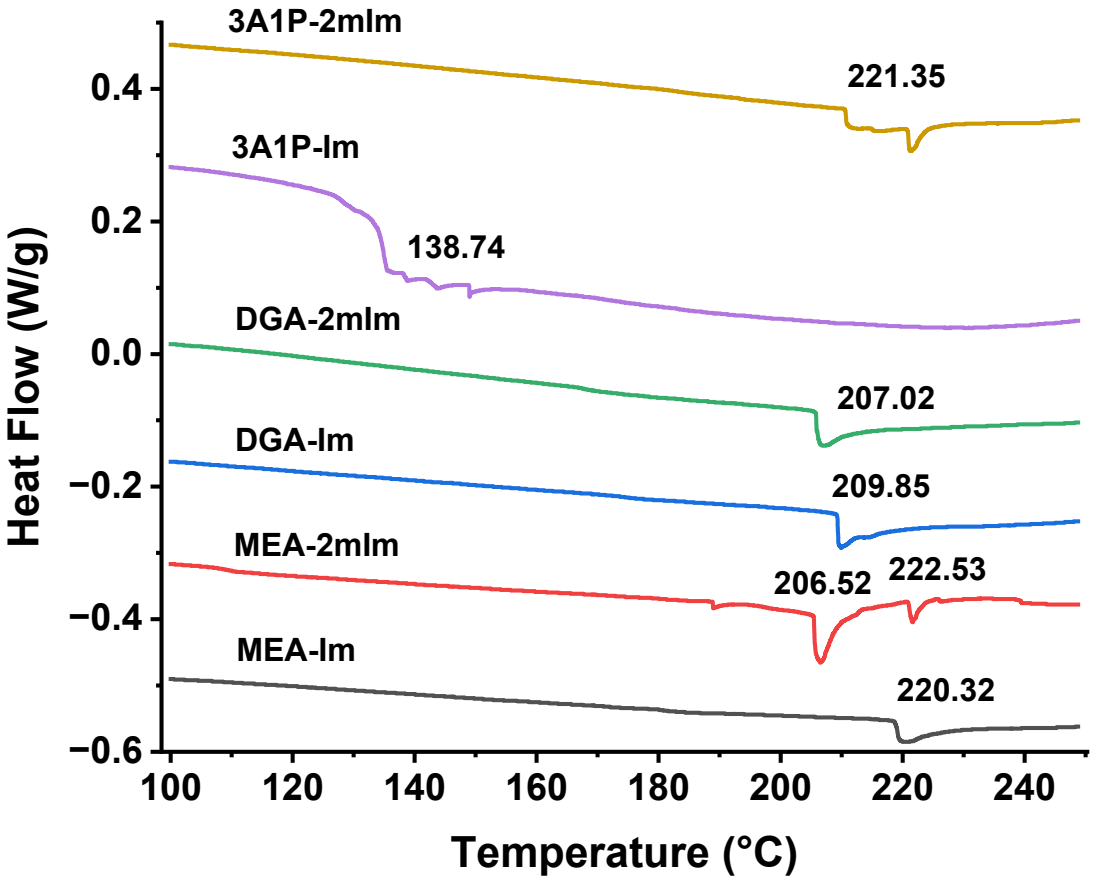

Fig. S 15 Endothermic melting peaks (T_m) of ionene-PAs.

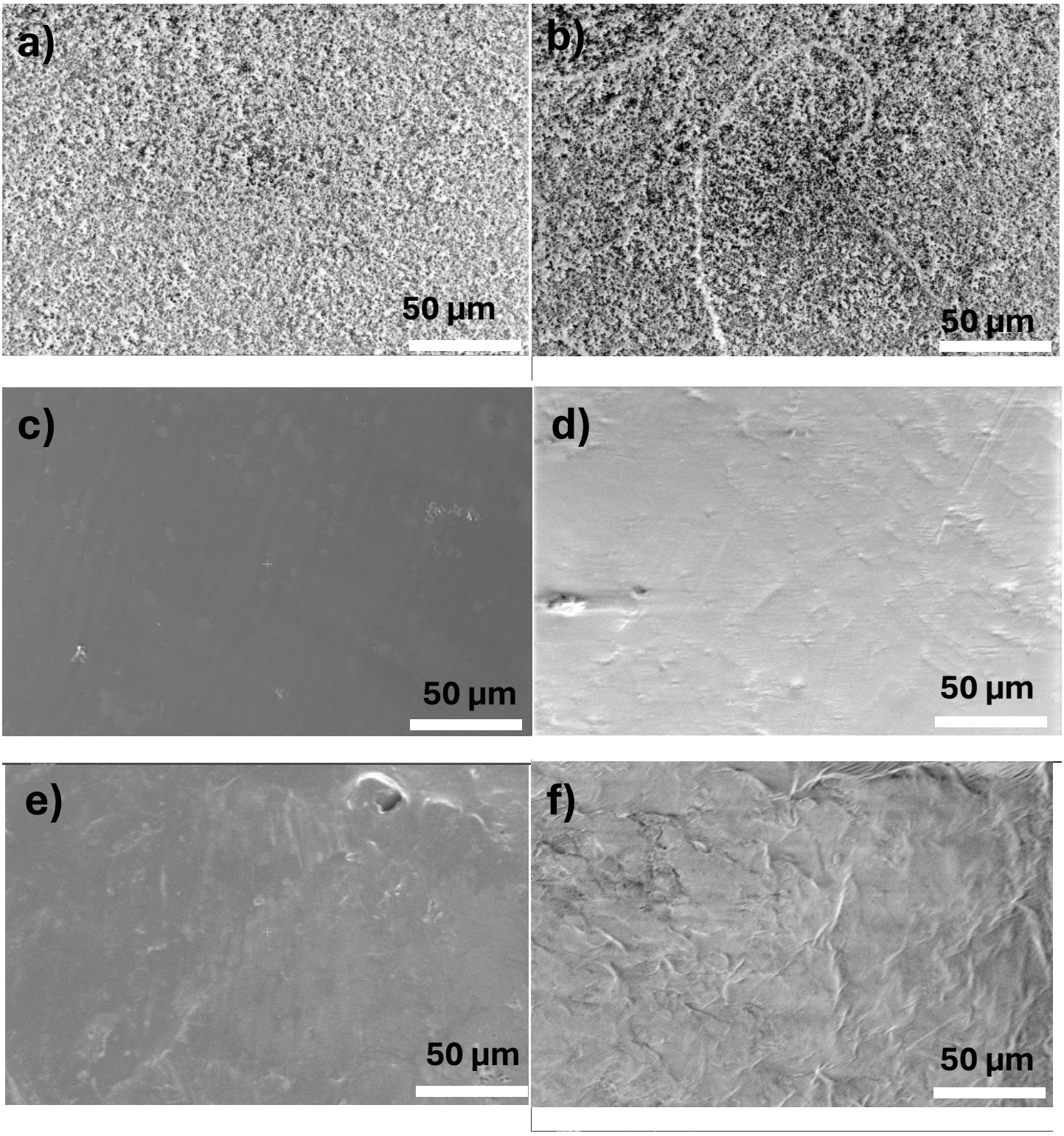

Fig. S 16 SEM images of neat ionenes a) MEA-im b) MEA-2mim c) 3A1P-im d) 3A1P-2mim e) DGA-im f) DGA-2mim

S6. Printability of ionenes and self-healing observed by SEM.

Fig. S 17 Extruded fiber and disc printed from DGA-im ionene.

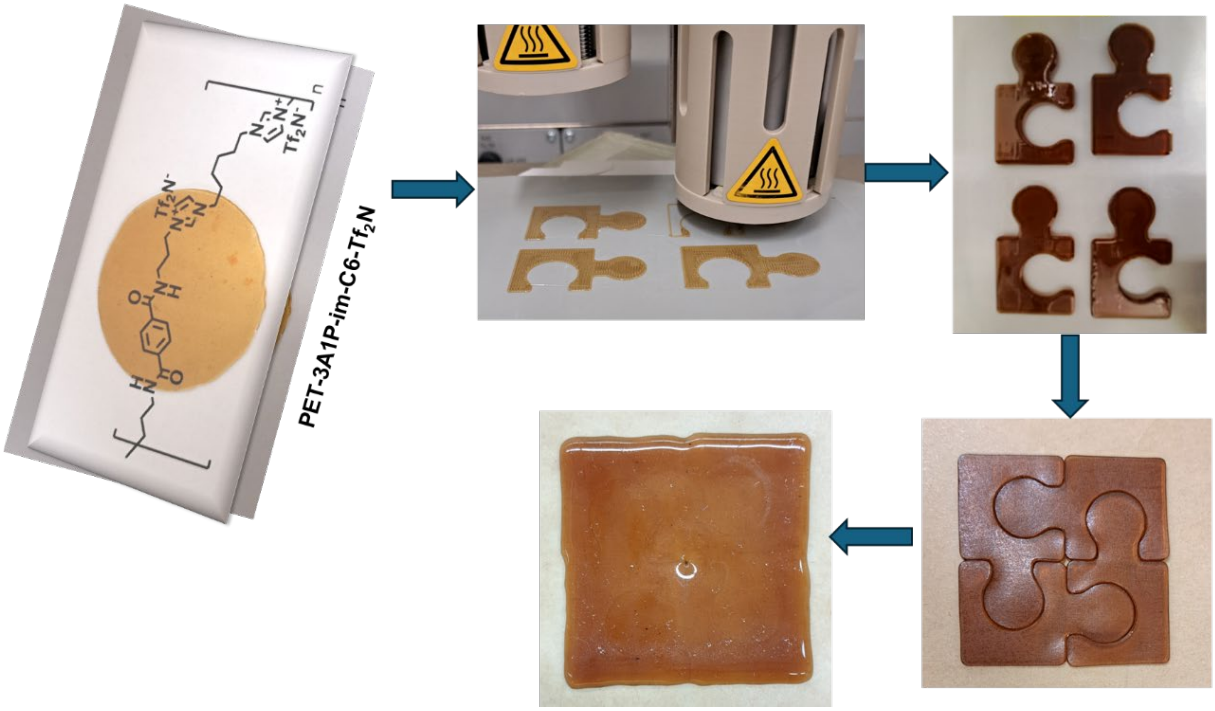

Fig. S 18 Four puzzle pieces prepared from 3A1P-im PA ionene gradually fusing via self-healing to a single shape.

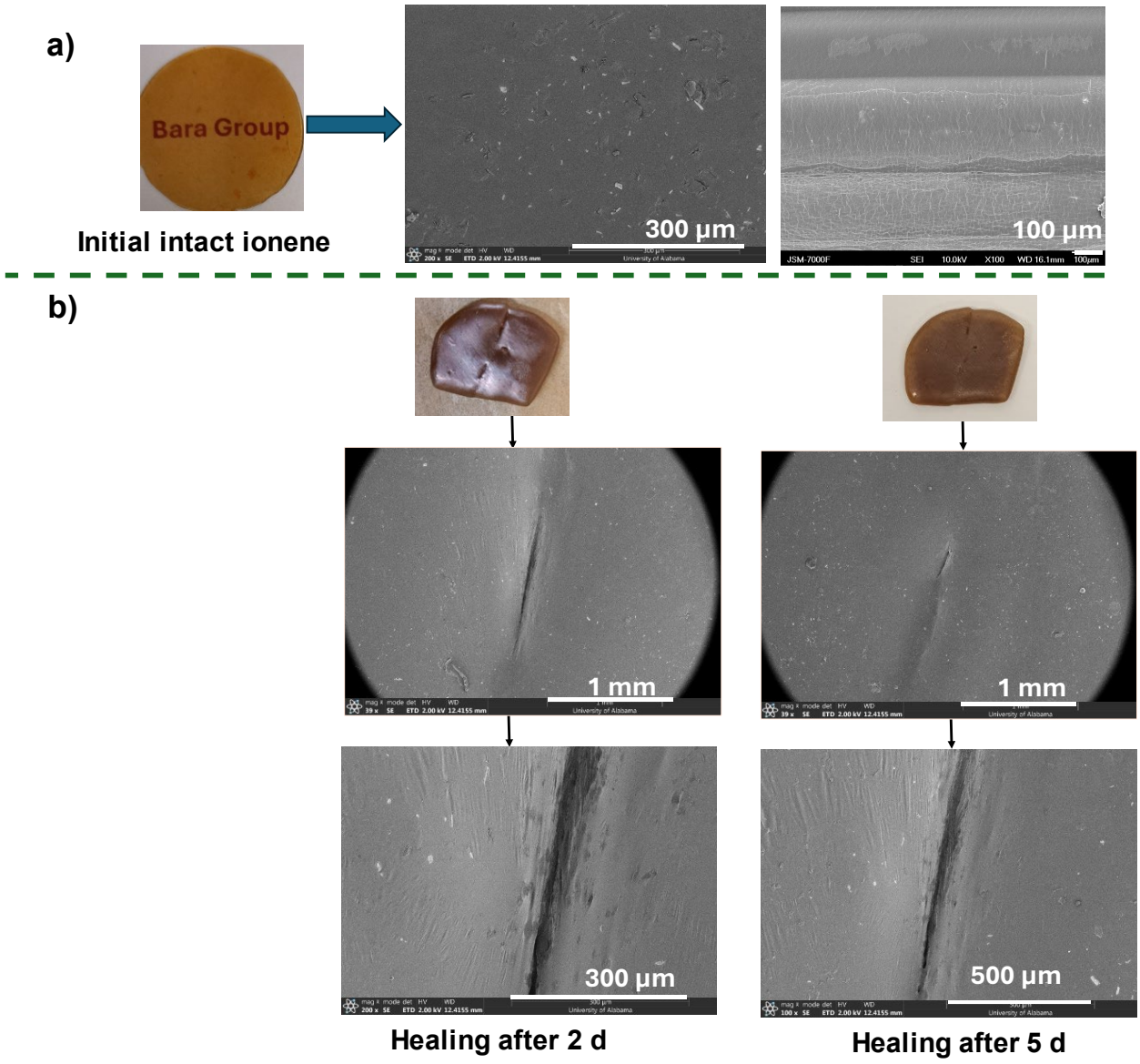

Fig. S 19 a) Images for thin film membrane prepared from 3A1P-im PA ionene and top surface image of the membrane by SEM. **b)** the adhered part of the midpoint cut ionene with the cross-sectional view of the self-healed images after 2 d and 5 d by SEM.

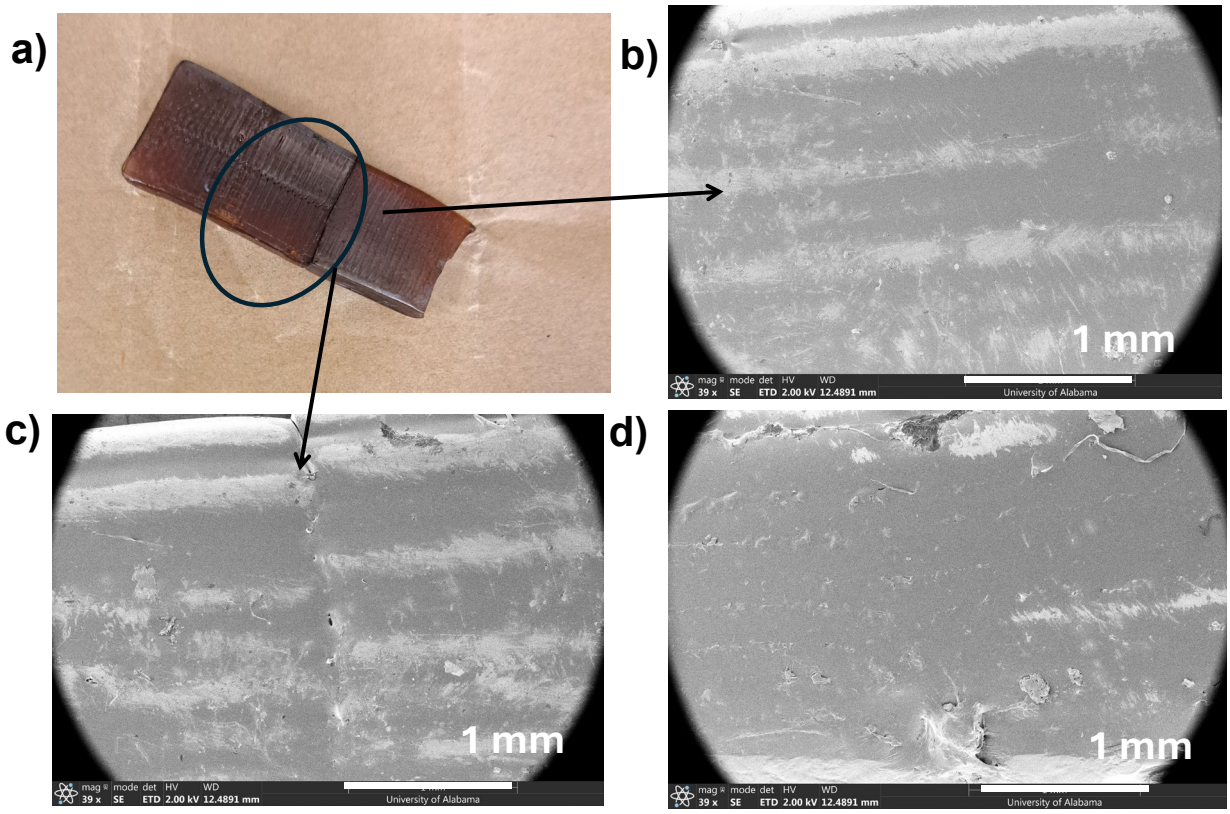

Fig. S 20 a) Part of 3D printed slab after tensile testing of 3A1P-2mim ionene. **b)** the infill pattern of the printed bar is unaffected by a cut or seam. **c)** cross-sectional view of the self-healed image of the slab from an intermediate seam restored after 4 days. **d)** edge of the self-healed slab.

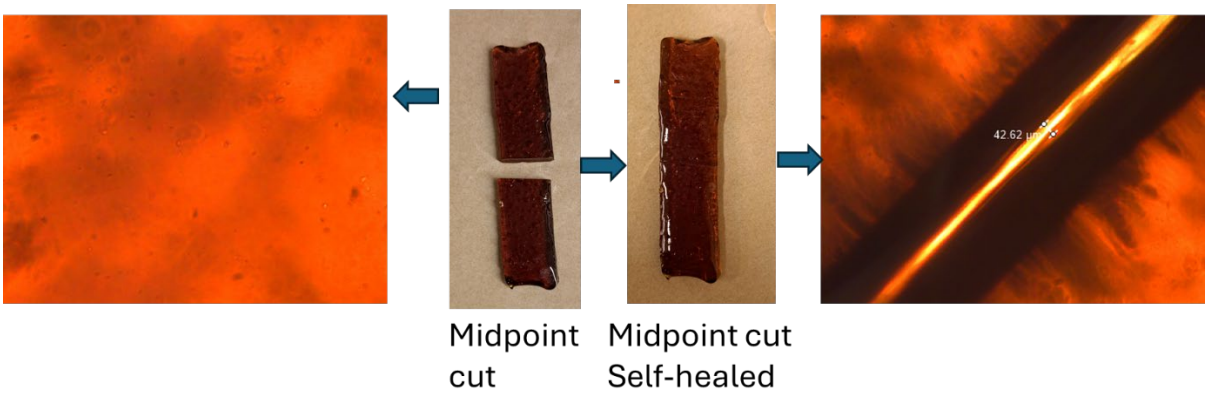

Fig. S 21 A melt-casted rectangular bar from 3A1P-2mim compound was cut in the center, and an optical image captured the self-healed seam after 4 days.

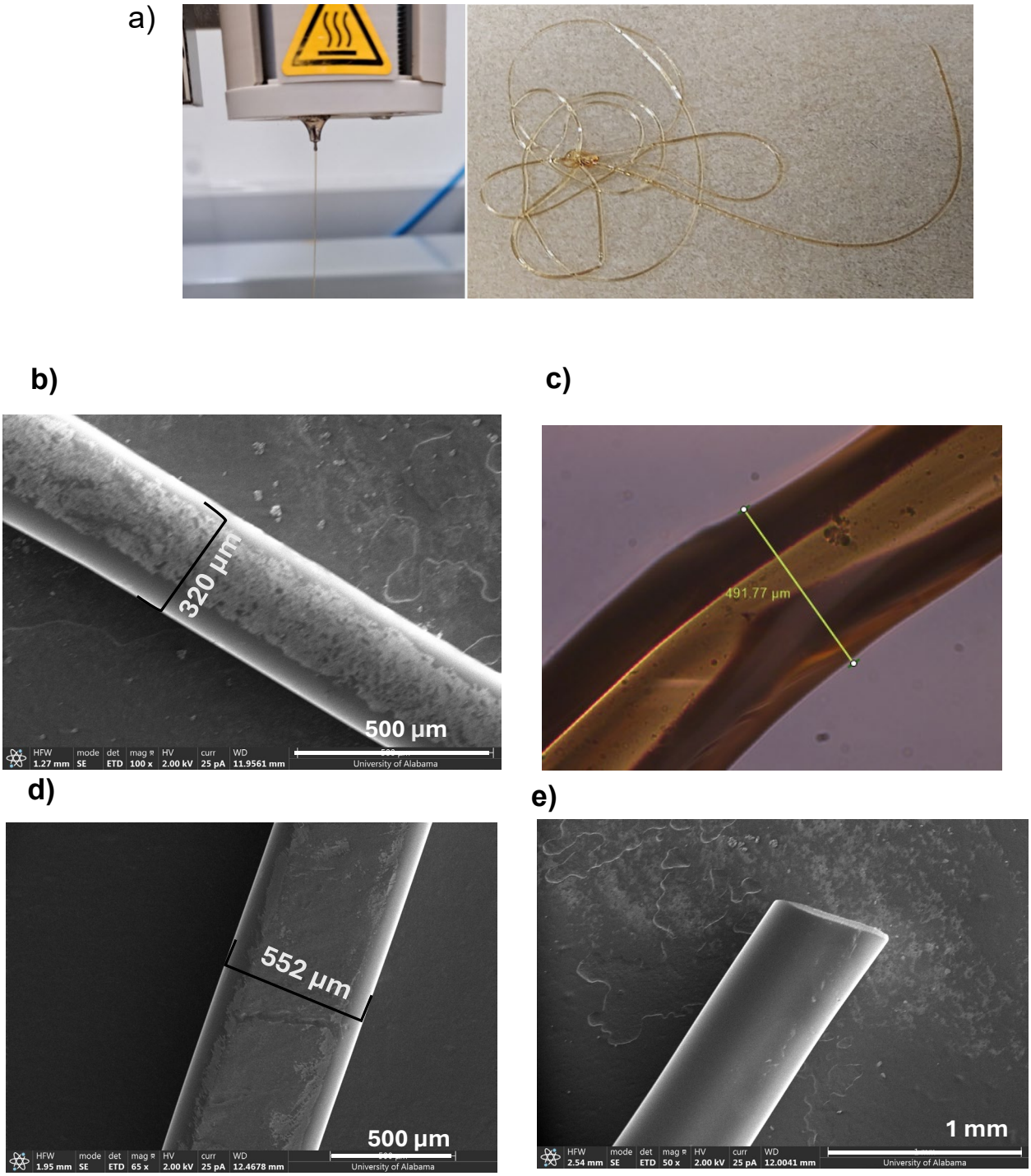

Fig. S 22 a) 3D printed single layer extruded filament by optical microscopy and SEM of different materials. **b)** 3A1P-im ionene **c)** MEA-2mim ionene + [C_4mim] [Tf_2N] IL. **d)** 3A1P-2mim e) edge of the fiber of 3A1P-2mim.

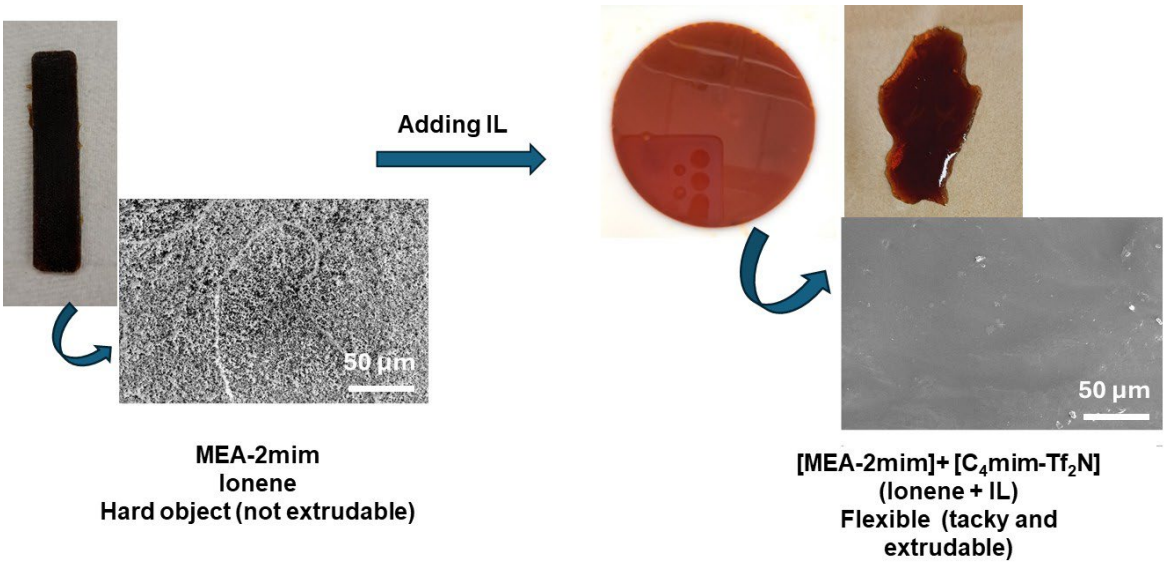

Fig. S 23 PET-MEA-2mim-C_6-Tf_2N (MEA-2mim) exhibiting a change in texture after adding [C_4mim] [Tf_2N] ionic liquid (IL).

S7. Mechanical property of PA-ionenes and demonstrating self-healing, shape memory (SM) and shape recovery behavior.

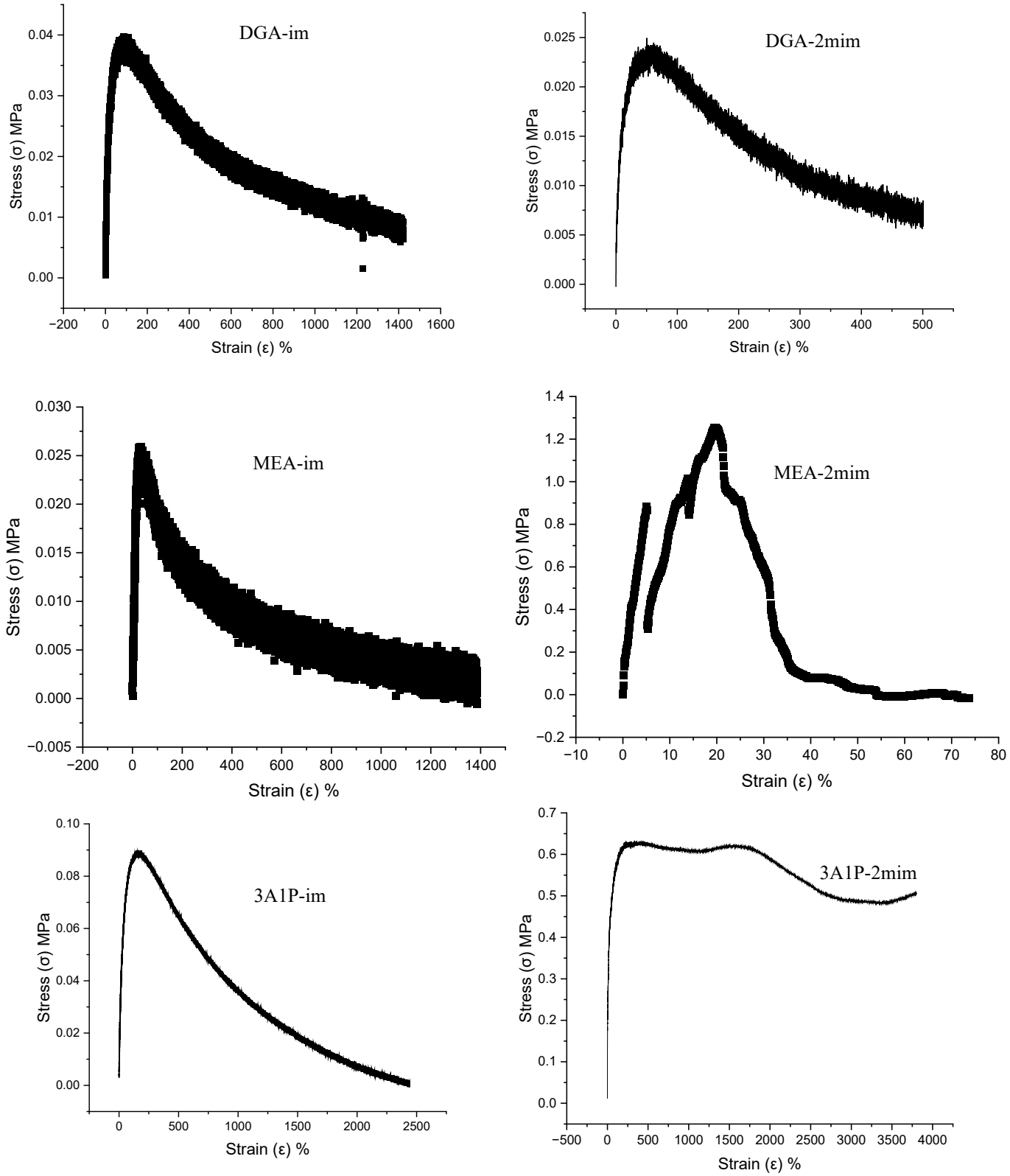

Fig. S 24 Full stress-strain curve of six different PA-ionenes.

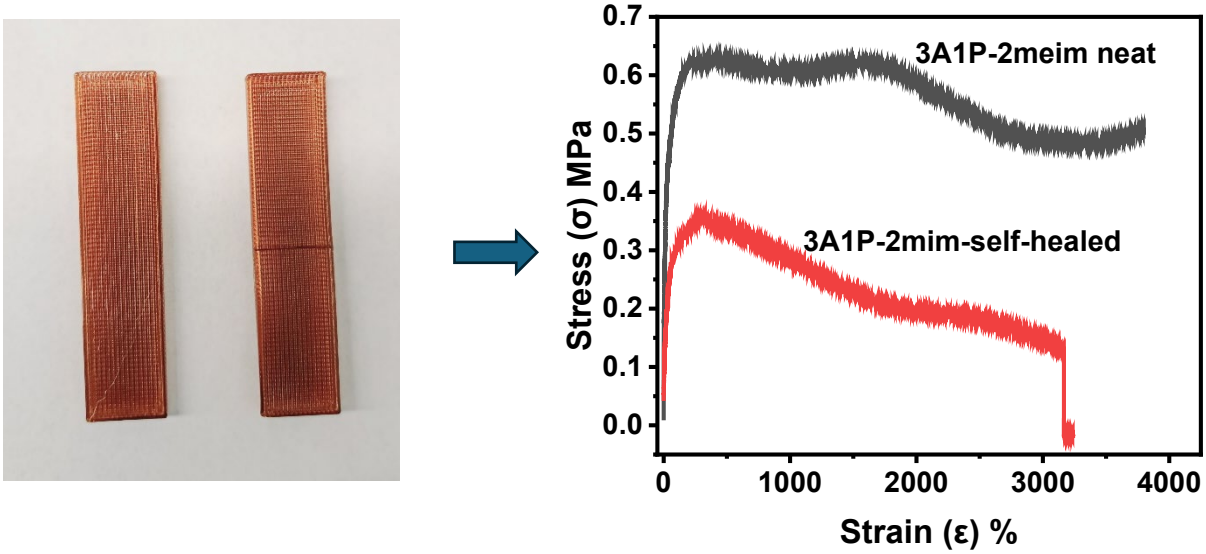

Fig. S 25 Self-healing after midpoint cut of 3A1P-2mim ionene printed slab.

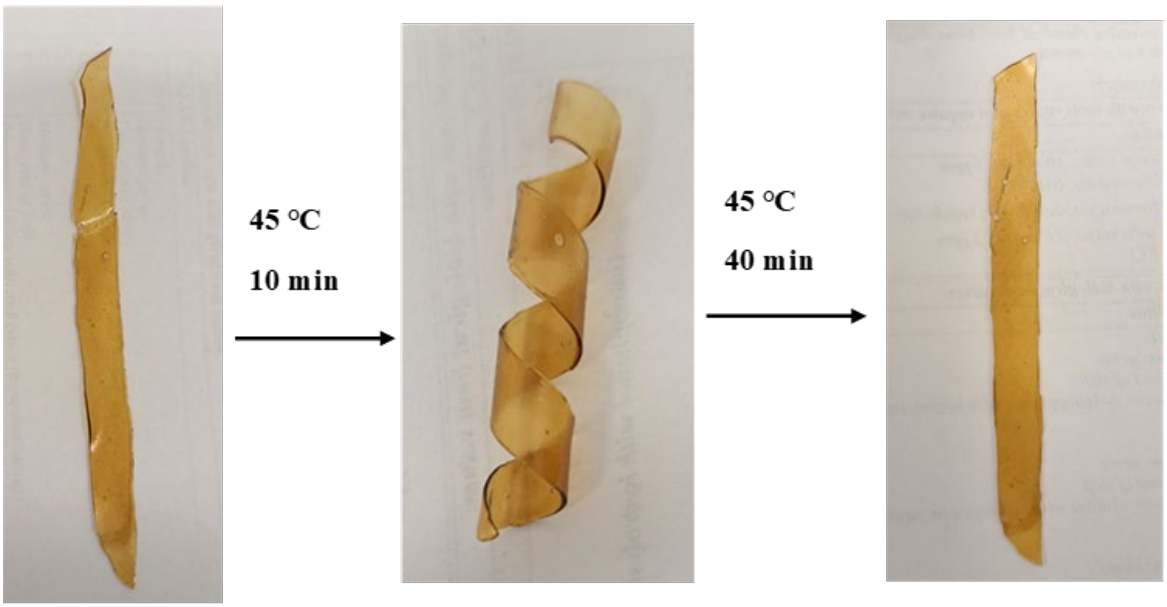

Fig. S 26 SM behavior observed by 3A1P-2mim ionene.

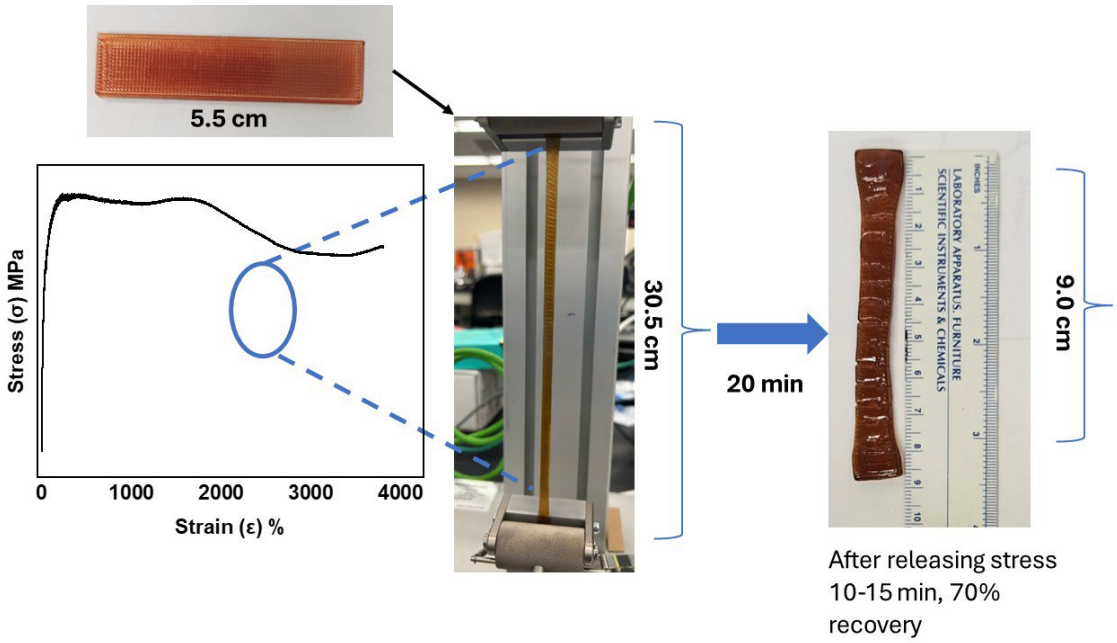

Fig. S 27 70% Shape recovery of 3A1P-2mim rectangular bar.